Research Journal of Applied Sciences, Engineering and Technology 5(13): 3508-3519, 2013
DOI:10.19026/rjaset.5.4479
ISSN: 2040-7459; e-ISSN: 2040-7467

Submitted: June 13, 2012 Accepted: July 04, 2012 Published: April 15, 2013

Research Article

Design and Simulation of Jet-driven Vascular Robot

Jiang Fan and Liu Zhenzhang
School of Mechanical and Electric Engineering, Guangzhou University,
Guangzhou, 510006, China

Abstract: For driven and adjustment attitude shortcomings of the existing vascular robot, a jet-driven vascular robot is designed, consists of the upper and lower shell, micro-batteries, variable pump, radio control block, 12 suction nozzles, 24 2/2-way solenoid valves and operation mechanism. The propel force of jet-driven, pressure in elastic capsule, propulsive efficiency and other parameters of vascular robot are analyzed, the propulsive efficiency is 41.6% in initial calculation. The flow path control method of robot posture adjustment in vascular is obtained. CFD technology is used to analyze the flows with capsule contraction and expansion of variable pump and the external flow field characteristics of vascular robot under the moving mode and the posture adjustment. The results show that the contraction and expansion of the variable pump can jet and suck the fluid, to drive vascular robot go straight in blood vessel, in the same time, the pressure field and velocity field under condition of pitch and roll, is met to the movement trend of the robot correspondingly.

Keywords: Dynamics mesh, jet-driven, numerical simulation, posture adjustment, propel force, variable pump, vascular robot

INTRODUCTION

The vascular robot for minimally invasive vascular diagnostic and vascular surgery has become a hot topic in the medical field, the study focus is propel approach of micro-robot. The propel modes been studied more are spiral rotating propulsion, the tail swinging propulsion, retractable imitation worms propulsion (Chen *et al*., 2010; Li, 2008). South Korean researchers have developed the vascular robot, which can move freely in the blood vessels and clear blood clots. This robot is driven by the external magnetic field, spin 20 to 30 times/sec, can move freely in coronary arteries, large veins and arteries etc., thick blood vessels and rotate to remove the blockage of blood vessels. In another example, Israeli scientists have developed a vascular robot with diameter of 1 mm, length 4 mm, the power of this robot comes from the excited vibration by the external magnetic field and with manipulator, could seize the vessel wall for crawling, also swim in the blood vessels, could be used as drug delivery tools for minimally invasive surgery and near-therapy in the treatment of cancer. In addition, Sweden, the United States, Germany, also developed a variety of vascular robot prototypes. China has also made more research in the vascular robot, for example, the patent with application No. 200410022740.1 discloses the vascular robot for the treatment of blood clots in blood vessels, the robot is also driven by outside the vascular magnetic, could swim forward and backward, steering and other activities. These robot's power source come from the external magnetic field, using magnetic properties with the same pole repulsion, the different pole attraction pole, by changing the external magnetic field, effecting magnetic force and magnetic torque, to control robot movement posture and position in the blood vessel, which makes the robot to work without time limit in blood vessels and help reduce the size of the robot, but the structure of the external magnetic field is complex and large, the control system is complex. Another example is patent applications with the application No. 200510040877.8, it opens a magnetic field-driven device and method used in body detector, which is a magnetic micro-robot driven by the external magnetic field, consist of the mobile bed, the drive coil sets outside of bed and the composition operator. The drive coil is made of the moving coil, the pitch coil and the deflection coil, which are layered each other. diagnosis and treatment operator could produce control commands for controlling the magnetic micro-robot moving, yaw, pitch and stop and these control instructions processed by the processing center, to control current, rotation of driven coil and the relative position between the coil and bed, thus produce the magnetic field to achieve a variety of micro-robot movement. Obviously, this structure of external magnetic field driven micro-robot is complex and not

Corresponding Author: Jiang Fan, School of Mechanical and Electric Engineering, Guangzhou University, Guangzhou, 510006, China

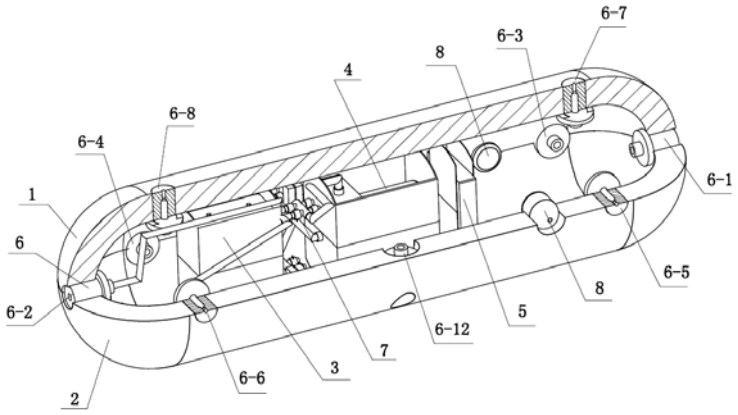

Fig. 1: The structure of jet-driven vascular robot
1: The upper shell; 2: The lower shell; 3: Micro-batteries; 4: Variable pump; 5: Radio control block; 6: Suction nozzles; 7: 2/2-way solenoid valves; 8: Operation mechanism

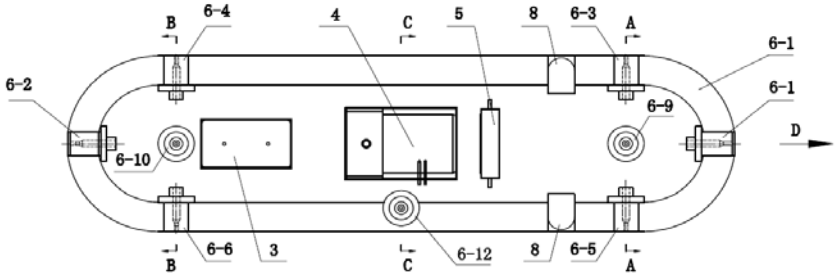

Fig. 2: The top view after removing the upper shell

easy to control (Kim *et al*., 2008; Jiang, 2010; Jiang *et al*., 2010a, b).

In this study, a new jet-driven micro-robot is designed based on shortcoming of driven approach in the existing vascular robot and drive parameters are analyzed, the control flow paths of walking and posture adjustment are obtained. The dynamic mesh technology is used to analyze the flow field of elastic capsule of variable pump under condition of the contraction and expansion, but also the flow field straight, pitch and roll condition, which is outside of vascular robot, is simulated, the analysis results is good reference for structure optimization of the vascular robot.

DESIGN OF JET-DRIVEN VASCULAR ROBOT

Structure design: Shown in Fig. 1 to 6, the jet-driven vascular robot is consist of the upper and lower shell, micro-batteries, variable pump, radio control block, 12 suction nozzles, 24 2/2-way solenoid valves and operation mechanism. Its diameter is 4 mm and it could swim in blood vessels of diameter 6 mm. Suction nozzle is key for swim and posture adjustment of vascular robot. Its shape is a cylinder, with an internal

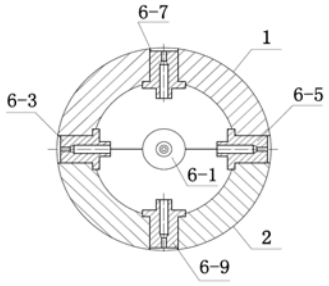

Fig. 3: A-A view

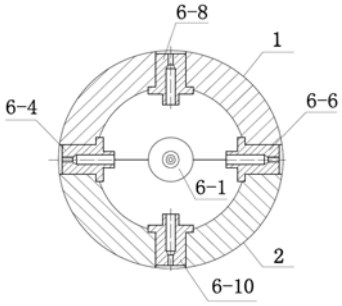

Fig. 4: B-B view

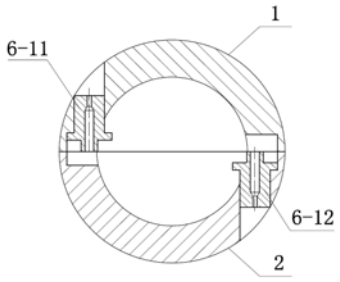

Fig. 5: C-C view

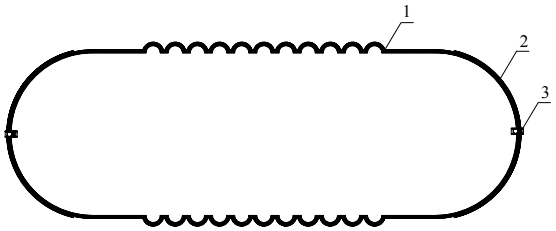

Fig. 6: The structure of variable bump
1: Corrugated ring; 2: Magnetic material; 3: One-way valve

axial through-hole, whose both ends tapered outward expansion, the taper length of the outer end is shorter than that of the inner end, the middle section is the downstream segment, in Fig. 2 to 6. 6-1 until 6-12 indicate the position of suction nozzle (Jiang, 2010).

Because the vascular robot swims in blood vessels, its components must be miniaturized. Micro-batteries mainly supplies energy for the wireless receiver control block and the operation mechanism, their volume should be less than 1mm in diameter. Variable pump uses the structure shown in Fig. 6, the main body is the elastic capsule structure with corrugated ring, magnetic material covering the surface outside of its end to squeeze and expansion the elastic capsule under the influence of external magnetic field, making the capsule volume changes and then suction or jet liquid. The operation mechanism is installed according to the needs, such as a manipulator is installed to clean up blood clots.

Principle of swimming and posture adjustment: The jet-driven principle of jet-driven vascular robot is similar to the jet-driven of the squid, variable pump in the vascular robot quickly ejects the blood, the jet flow is faster than blood flow, blood vessels, so give the robot a reverse thrust, this reverse thrust to drive the robot forward. The propulsive efficiency of vascular robot is analyzed by following.

The actual filling liquid volume of variable pump in vascular robot is the internal volume variation V in this time, the momentum variation of the liquid ejected per unit time is propel force, under unsteady conditions, the propel force is calculation by the following equation (Du, 2008):

$$F(t) = \frac{\partial}{\partial t}\int_{CV} u_j(x,t)\rho dV + \int_{CS} u(x,t)\rho u_j(x,t)dA \quad (1)$$

where,
F(t) : The propel force produced by jet flow at time t
P : The density of blood
$u_j(x, t)$: Velocity of jet flow by vascular robot
dv : Volume increment of elastic capsule in the variable pump
dA : Area increment of internal surface of the variable pump

Equation (1) is more complex to calculate the propel force F(t), but only consider the quasi-steady flow, the propel force F(t) can be simplified to Eq. (2):

$$F(t) = \rho A_n u_j^{\ 2} \quad (2)$$

where, A_n is internal section area of suction nozzle:

$$A_n = \frac{\pi D_n^{\ 2}}{4}$$

D_n : Nozzle diameter
u_j : Velocity of jet flow

According to the Bernoulli equation of the unsteady flow, the pressure inside of elastic capsule of variable pump could be drawn when the vascular robot swims, such as the Eq. (3):

$$z_m + \frac{p_m}{\rho g} + \frac{u_m^{\ 2}}{2g} = z_j + \frac{p_j}{\rho g} + \frac{u_j^{\ 2}}{2g} + \frac{1}{g}\int_{s_0}^{s_j} \frac{\partial u(s,t)}{\partial t} ds \quad (3)$$

where,
z_m : The blood depth inside of elastic capsule
z_j : The depth of jet flow related the reference point
p_m : The pressure inside of elastic capsule
p_j : The pressure of jet flow
u_m : Flow velocity inside of elastic capsule
u(s, t) : Flow velocity inside of control volume
s : The streamline length from the variable pump to suction nozzle, that is from s_0 to s_j

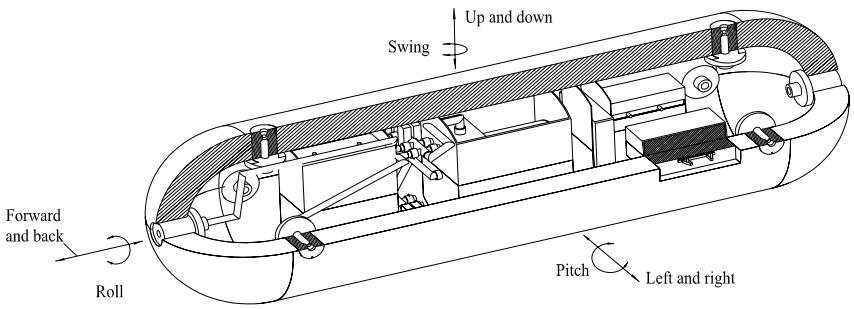

Fig. 7: The posture of vascular robot

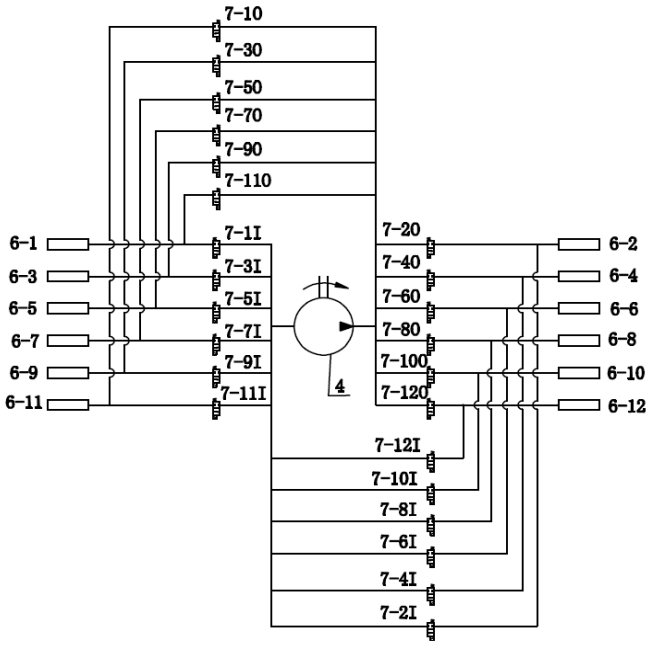

Fig. 8: The connection relationship among of suction nozzle, variable pump and solenoid valve in vascular robot

The loss induced by the fourth item in the right of Eq. (3) is very small, can be ignored in only consider quasi-steady flow. Assume that vascular robot swimming follows the horizontal direction and jet flow is also along the horizontal direction, p_j is approximately 0, the pressure inside of elastic capsule of variable pump can be calculated by Eq. (4):

$$p_m = \frac{\rho u_j^{\,2}}{2} \tag{4}$$

When the angle between the nozzle axis of the robot and the swimming direction is known, the propulsive efficiency of the robot can be calculated by Eq. (5):

$$\eta_j = \frac{TU\cos\theta}{TU\cos\theta + \frac{\rho V}{2t}[(u_j\cos\theta - U)^2 + u_j^{\,2}\sin^2\theta]} = \frac{2Uu_j\cos\theta}{U^2 + u_j^{\,2}} \tag{5}$$

where,
U: Swim velocity of vascular robot
V: The volume of elastic capsule of variable pump

As the blood density is 1.056 g/cm^3, vein blood flow is 12 cm/s, the volume of elastic capsule of variable pump is 56.55 mm^3, nozzle diameter is 0.5 mm, u_j is 14.4 cm/s, the angle θ between the nozzle axis of the robot and the swimming direction is 0, the robot moving velocity U is 3 mm/s, then the propulsive force is 0.0062 N calculated by (2), (4), (5), the pressure

inside of elastic capsule is 10.95 Pa, the propulsive efficiency η_j is 41.6%.

The fluid flow path analysis under vascular robot swimming and posture adjustment: Figure 7 is a posture diagram of jet-driven vascular robot, vascular robot suspended in the blood has six degrees of freedom, could achieve 12 swimming actions.

The connection relationship among of suction nozzle, variable pump and solenoid valve in vascular robot is shown in Fig. 8. Vascular robot achieves the movement shown in Fig. 7, by through connection and disconnection between of different suction nozzle and the entrances and exits of the variable pump. Under the different posture of vascular robot, the connection and disconnection between of suction nozzle and variable pump, open and closed of solenoid valve are described in detail below (Jiang, 2010).

Forward: The solenoid valve 7-1I, 7-2O open, blood enter the variable pump 4 from the pump suction nozzle 6-1 and jet by the suction nozzle 6-2, drive the robot swim forward (Fig. 2 in the direction of the arrow D).

Backward: The solenoid valve 7-2I, 7-1O open, blood enter the variable pump 4 from suction nozzle 6-2 and jet by the suction nozzle 6-1, drive the robot swim backwards.

Upward translation: The solenoid valve 7-7I, 7-8I, 7-9O and 7-10O open, blood enter the variable pump 4 from the suction nozzle 6-7, 6-8 and jet by the suction nozzle 6-9, 6-10 and drive the robot to upward translation.

Downward translation: The solenoid valve 7-9I, 7-10I, 7-7O and 7-8O open, blood enter the variable pump 4 from suction nozzle 6-9, 6-10 and jet by the suction nozzle 6-7, 6-8, drive the robot to downward translation.

Left translation: The solenoid valve 7-3I, 7-4I, 7-5O and 7-6O open, blood enter the variable pump 4 from the suction nozzle 6-3, 6-4 and jet by the suction nozzle 6-5, 6-6, drive robot to left translation.

Right translation: The solenoid valve 7-5I, m7-6I, 7-3O and 7-4O open, blood enter the variable pump 4 from the suction nozzle 6-5, 6-6 and jet by the suction nozzle 6-3, 6-4, drive the robot to right translation.

Front left tilt: The solenoid valve 7-6I, 7-5O open, blood enter the variable pump 4 from the suction nozzle 6-6 and jet by the suction nozzle 6-5, drive the robot to front left tilt.

Front right tilt: The solenoid valve 7-3I, 7-4O open, blood enter the variable pump 4 from the suction nozzle 6-4 and jet by the suction nozzle 6-3, drive the robot to front right tilt.

Front upward tilt: The solenoid valve 7-10I, 7-9O open, blood enter the variable pump 4 from the suction nozzle 6-10 and jet by the suction nozzle 6-9, drive the robot to front upward tilt.

Front downward tilt: The solenoid valve 7-8I, 7-7O open, blood enter the variable pump 4 from the suction nozzle 6-8 and jet by the suction nozzle 6-7, drive the robot to front downward tilt.

Clockwise rotation around the vertical axis: The solenoid valve 7-12I, 7-11O open, blood enter the variable pump 4 from the suction nozzle 6-12 and jet by the suction nozzle 6-11, drive the robot to clockwise rotation around the vertical axis.

Counterclockwise rotation around the vertical axis: The solenoid valve 7-11I, 7-12O open, blood enter the variable pump 4 from the suction nozzle 6-11 and jet by the suction nozzle 6-12, drive the robot to counterclockwise rotation around the vertical axis.

NUMERICAL SIMULATION OF OUTSIDE FLOW FIELD OF THE JET-DRIVEN VASCULAR ROBOT

The motion performance of robot is required to analyze in vascular robot design and its shape is optimized. The experimental method is relatively expensive and relatively long period. Using CFD (Computational Fluid Dynamics) technology could obtain a variety of flow field data, such as force, torque and flow parameters of the vascular robot under any condition in the computer by solving the simplify basic equations of fluid dynamics between robot vessels and vascular wall, Thus provide reference data for motion parameters and the robot outer structure optimization. This study analyzes jet state of variable pump by use of moving mesh methods and the flow field under condition of the vascular robot is in straight, pitch, roll, swing and other working conditions.

Governing equations and computational model: As main body of the robot is cylindrical, which is the middle of the cylinder, both ends are the hemisphere, is similar as the capsule shape, the continuity equation and the N-S equations of the fluid flow between the

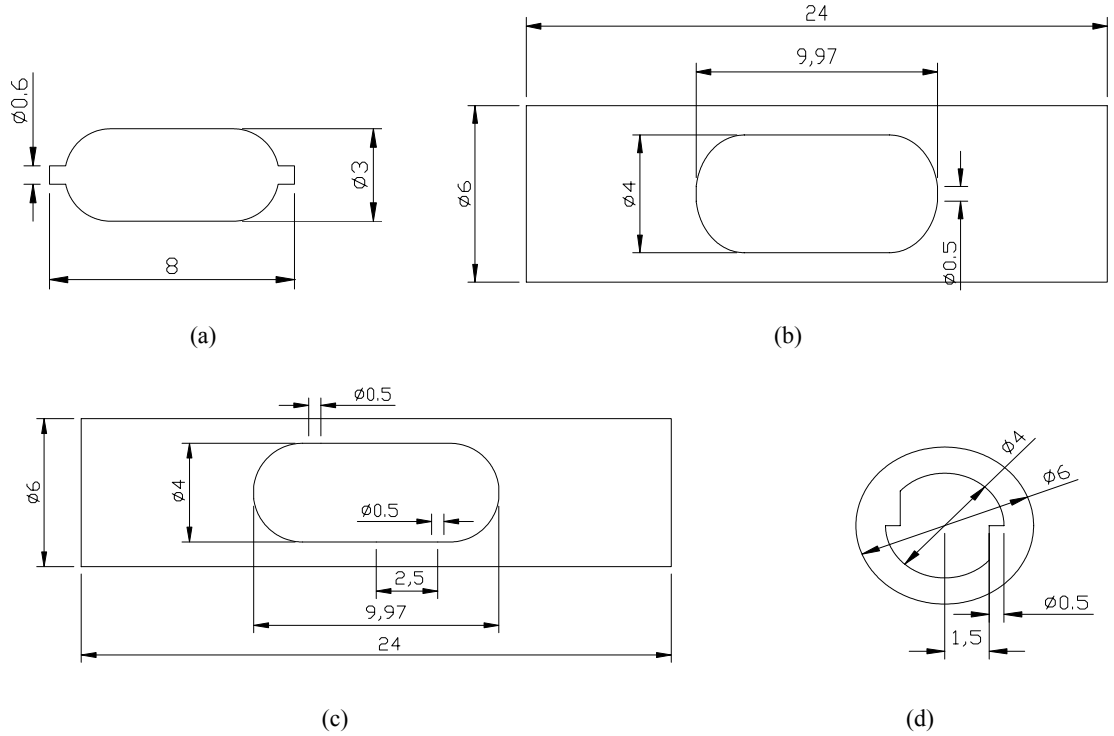

Fig. 9: The calculation models

blood vessels wall and vascular robot established under cylindrical coordinates, turbulence is calculated by standard k - □ model. the movement deformation of elastic capsule cavity in variable pump is achieved by using dynamic mesh, mesh update method is using by local remeshing (Jiang *et al*., 2010b, c, d, e; Jiang and He, 2012):

$$\frac{\partial(ru_r)}{\partial r}+\frac{\partial(ru_z)}{\partial z}=0 \quad (6)$$

$$\frac{\partial u_r}{\partial t}+u_r\frac{\partial u_r}{\partial r}+u_r\frac{\partial u_r}{\partial z}-\frac{u_\theta^2}{r}+\frac{1}{\rho}\frac{\partial p}{\partial r}=\mu(\nabla^2 u_r-\frac{u_r}{r^2}) \quad (7)$$

$$\frac{\partial u_\theta}{\partial t}+u_r\frac{\partial u_\theta}{\partial r}+u_z\frac{\partial u_\theta}{\partial z}+\frac{u_r u_\theta}{r}=\mu(\nabla^2 u_\theta-\frac{u_\theta}{r^2}) \quad (8)$$

$$\frac{\partial u_z}{\partial t}+u_r\frac{\partial u_z}{\partial r}+u_z\frac{\partial u_z}{\partial z}+\frac{1}{\rho}\frac{\partial p}{\partial z}=\mu\nabla^2 u_z \quad (9)$$

where,
u_r : Radial velocity
u_θ : Tangential velocity
u_z : Axial velocity
p : Pressure
μ : Viscosity

In order to simplify the calculation, the symmetry structure of capsule vascular robot is considered, the flow field on the symmetrical plane and the special cross-section plane is analyzed. Figure 9 shows the geometric models of calculation:

- The flow field analysis model under condition of elastic capsule contraction and expansion
- A model for the vascular robot straight swimming
- A model for the vascular robot under condition of pitch
- A model of the vascular robot under condition of roll. In the following numerical simulation, the blood density is 1056 kg/m^3, viscosity is 0.004 Pa.s.

Flow field numerical simulation of contraction and expansion of elastic capsule on the variable pump: Since the variable pumps elastic capsule is in motion during the contraction and expansion, dynamics mesh technology is used, the body shell at both ends of bowl-shaped elastic capsule is set as the movement body, the middle column and the tube of both ends are deformed. Contraction condition, the initial mesh parameters are: 4506 cells, 2352 nodes, as shown in Fig. 10a, the deformed mesh is shown in Fig. 10b, the mesh

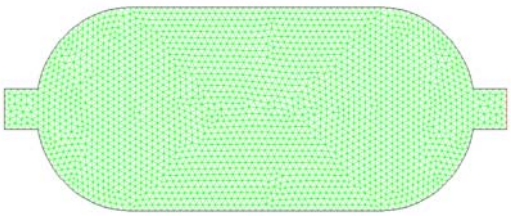

(a) Before contraction

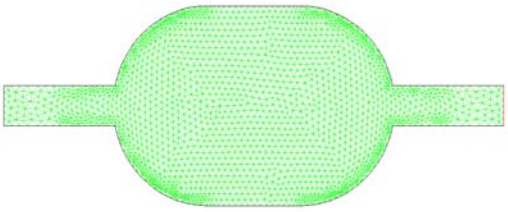

(b) After contraction

Fig. 10: The elastic capsule is under contraction

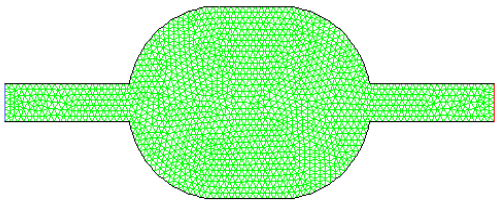

(a) Before expansion

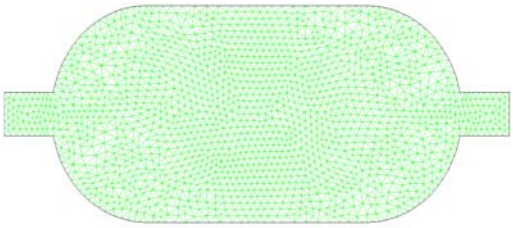

(b) After expansion

Fig. 11: The elastic capsule is under expansion

parameters: 4486 cells, 2345 nodes, from Fig. 9 and the mesh parameters variation, in contraction process, elastic capsule volume shrinking, the number of nodes and cells reduce. Expansion conditions, the initial mesh parameters are: 2910 cells, 1554 nodes, as shown in Fig. 11a, the deformed mesh is shown in Fig. 11b, the mesh parameters: 3458 cells, 1820 nodes, Fig. 10 and the mesh parameters variation show, in the expansion simulation, the elastic capsule volume expanding, the number of cells and nodes increase.

Under contraction condition at 25s, the pressure field and velocity field are shown in Fig. 12. See from the figure, elastic capsule contraction, pressure increases inside of elastic capsule, the maximum pressure reached 5.27 Pa, when the pressure is greater than the lock pressure of the exit one-way valve, liquid inside of elastic capsule ejected from the exit, the maximum jet velocity of 0.45 m/s.

Under expansion condition at 25s, the pressure field and velocity field are shown in Fig. 13. See from the figure, elastic capsule expansion, pressure reduces sharply, the minimum pressure of -5.16 Pa, when the pressure is less than the locking pressure of inlet one-way valve, liquid capsule sucked from inlet, the maximum suction velocity of 0.41 m/s.

Seen from the above simulation results, during elastic capsule contraction and expansion, it could jet the liquid and suck liquid, jet flow velocity is greater to drive the robot swimming forward.

Flow field numerical simulation under robot swim straight: Main resistance is blood flow resistance when vascular robots straight, by simulating the blood flow field outside of vascular robot, the forward resistance of vascular robot is obtained and the data is provided for shape optimization of vascular robot. The Fig. 8b is mesh of the computational domain, which are 23838 cells and 12342 nodes. The results are shown in Fig. 14:

- The pressure field results as the vascular robot move forward in the blood vessel, the pressure on the front-end is greater, the domain is closer to the axis of the robot, the pressure is greater.
- The velocity field results, the front-end and back-end have jet, the flow velocity is greater, the flow velocity on the domain between the vessel and the robot is also large.
- A pressure distribution curve on the front-end and back-end as robot straight swims, the domain is closer to axis of the robot the front, the pressure is larger, while that of back-end is the opposite.
- Velocity distribution curve on the front-end and back-end, as the robot uniform motion, the flow velocity of front-end and back-end is similar.

Flow field numerical simulation under robot posture adjustment: The vascular robot in blood vessels has six degrees of freedom, can have 12 postures, here only simulates two postures adjustment, is the pitch conditions Fig. 9c and the roll condition (Fig. 9d).

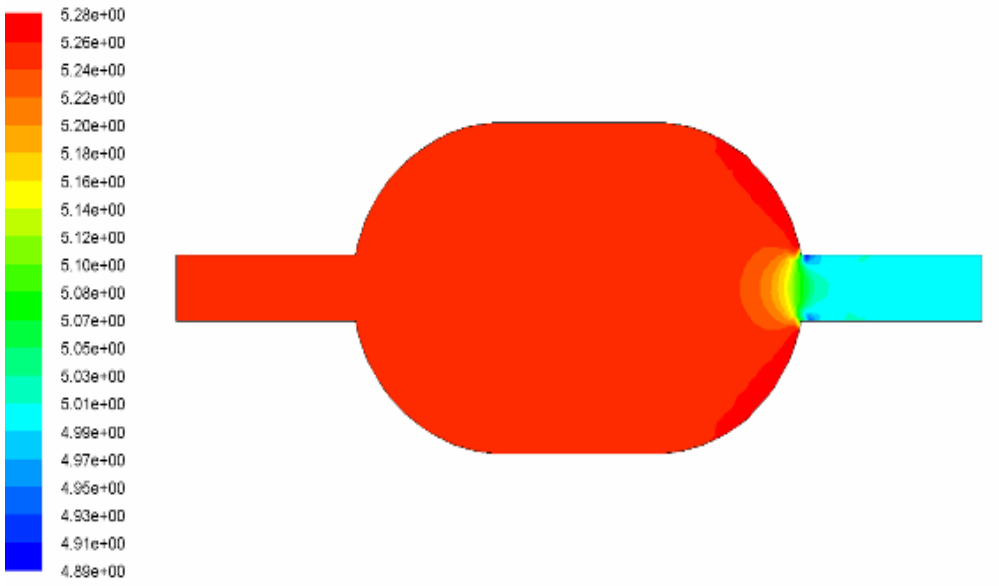

(a) The pressure field

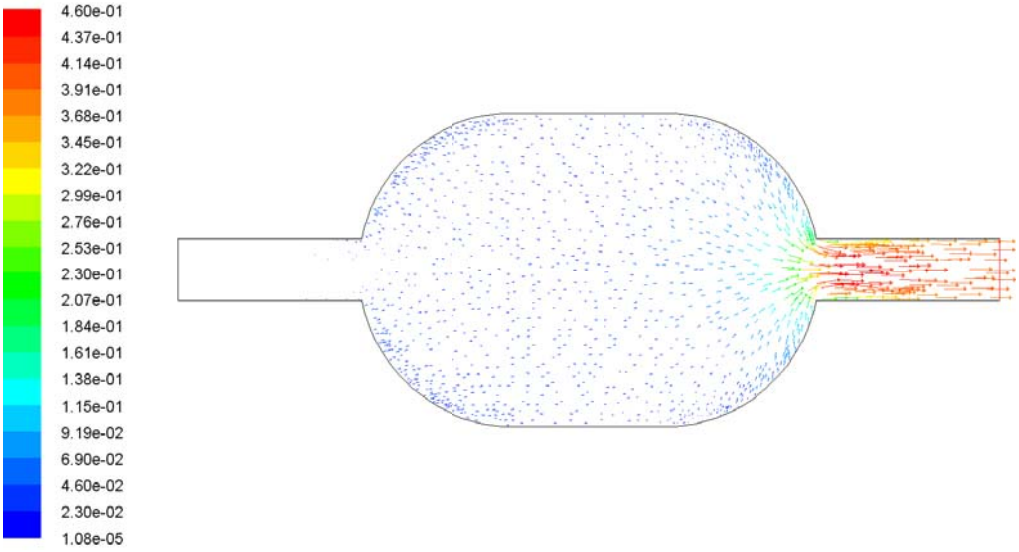

(b) The velocity field

Fig. 12: The pressure and velocity results inside of elastic capsule under condition of contraction

As the robot is under pitch conditions, the mesh parameters of computational domain are: 24530 cells, 12689 nodes. The results are shown in Fig. 15.

Figure 14, the vascular robot will bend front and rise back, the pressure on the bottom of the front is greater, the pressure the upper of the back is smaller; the bottom of the back has larger jet velocity, the upper of the front has greater liquid suck velocity.

When the vascular robot is in roll condition, a cross-sectional domain is taken as calculated domain, as shown in Fig. 9d. The mesh parameters of the computational domain: 3632 cells, 1976 nodes. The results are shown in Fig. 16.

Figure 16 shows the vascular robot has a counterclockwise rotation trends, the bottom liquid is squeezed, pressure increases and pressure on the upper

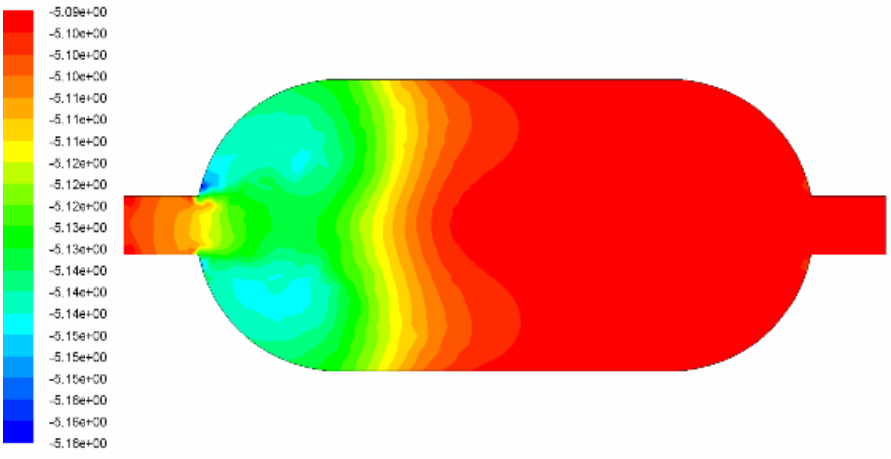

(a) The pressure field

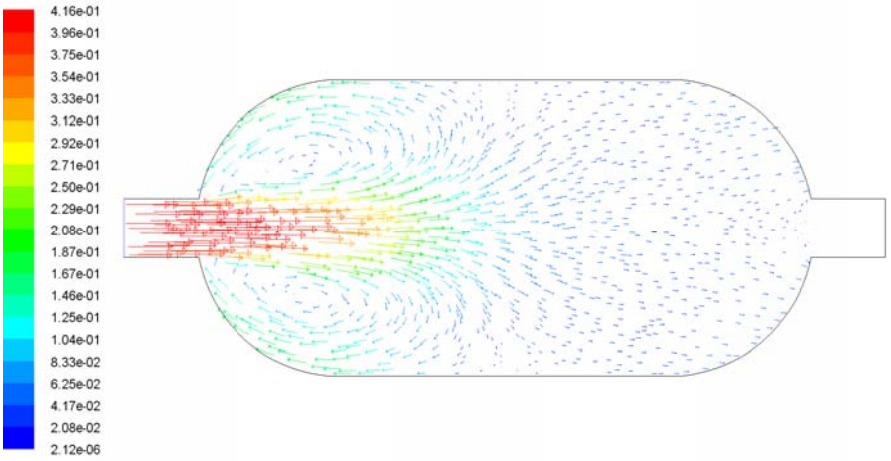

(b) The velocity field

Fig. 13: The pressure and velocity results inside of elastic capsule under condition of expansion

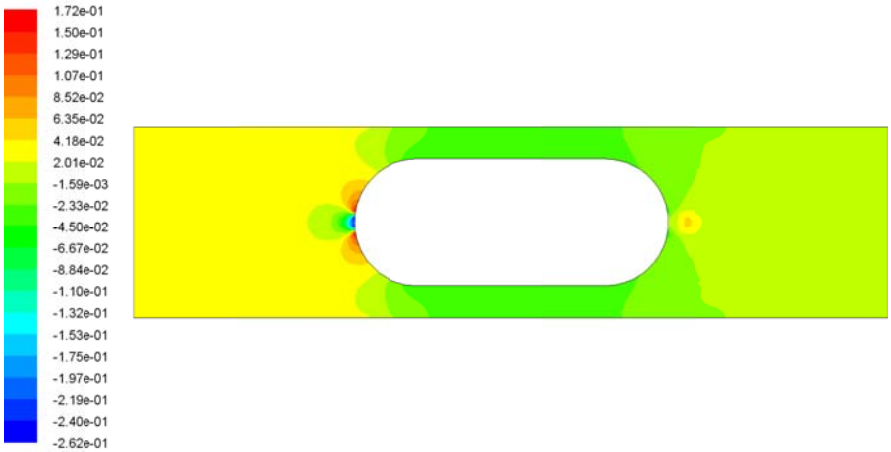

(a) The pressure field

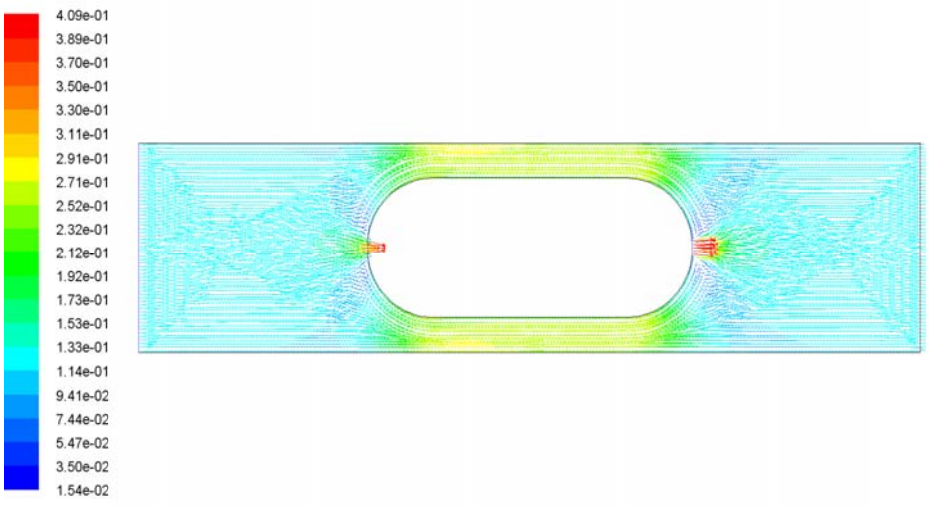

(b) The velocity field

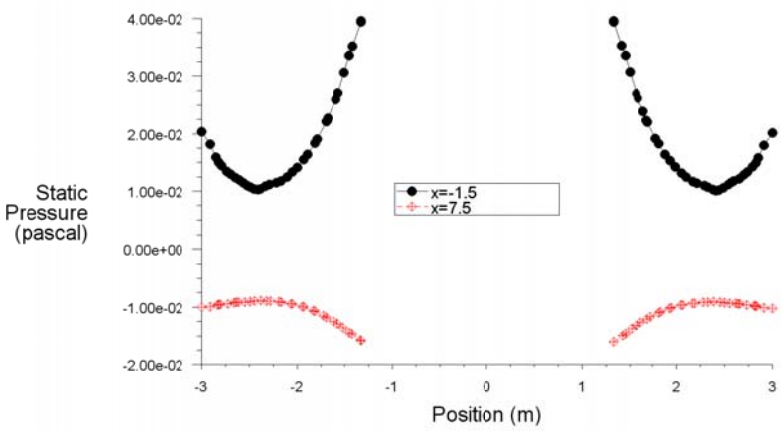

(c) The pressure curve at front-end and back-end

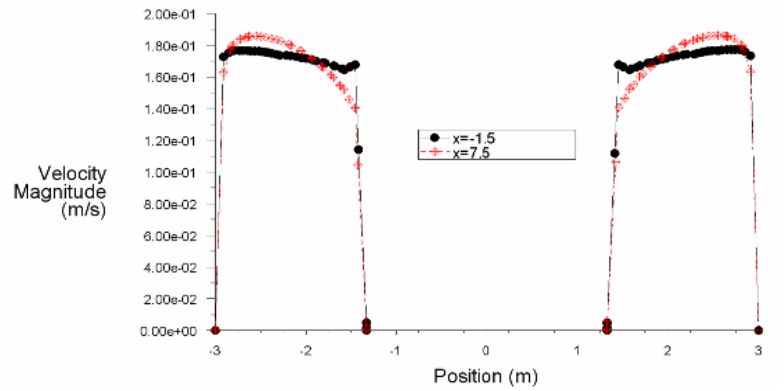

(d) The velocity curve at front-end and back-end

Fig. 14: The pressure and velocity results as vascular robot straight swims

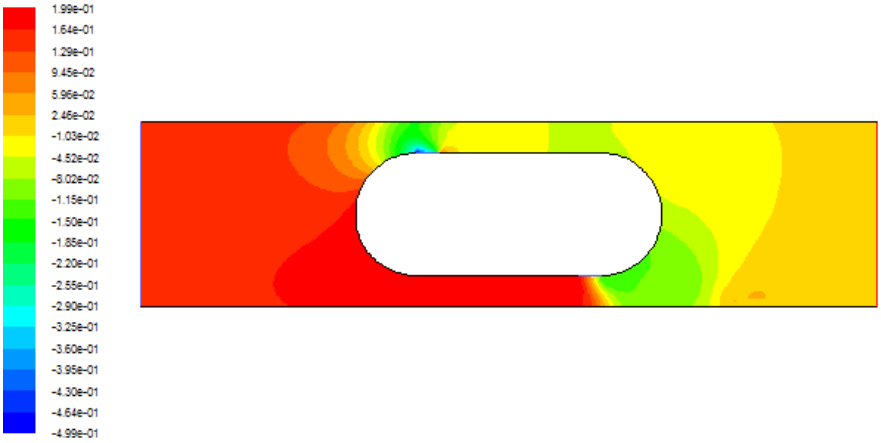

(a) The pressure field

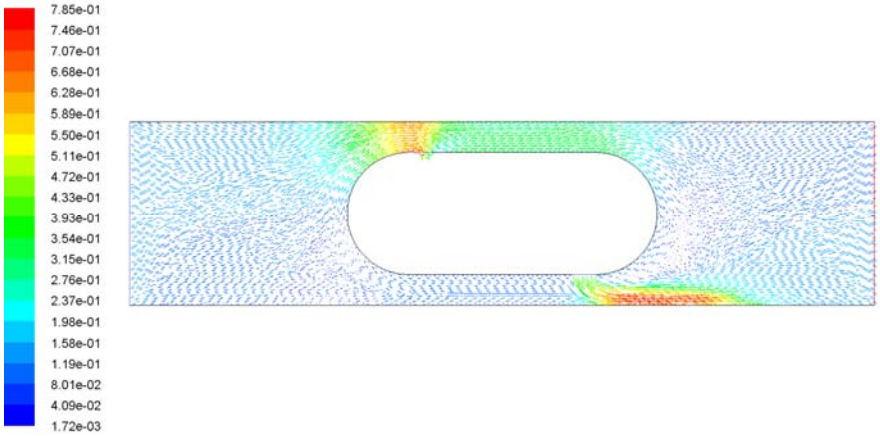

(b) The velocity field

Fig. 15: The results as vascular robot is under pitch conditions

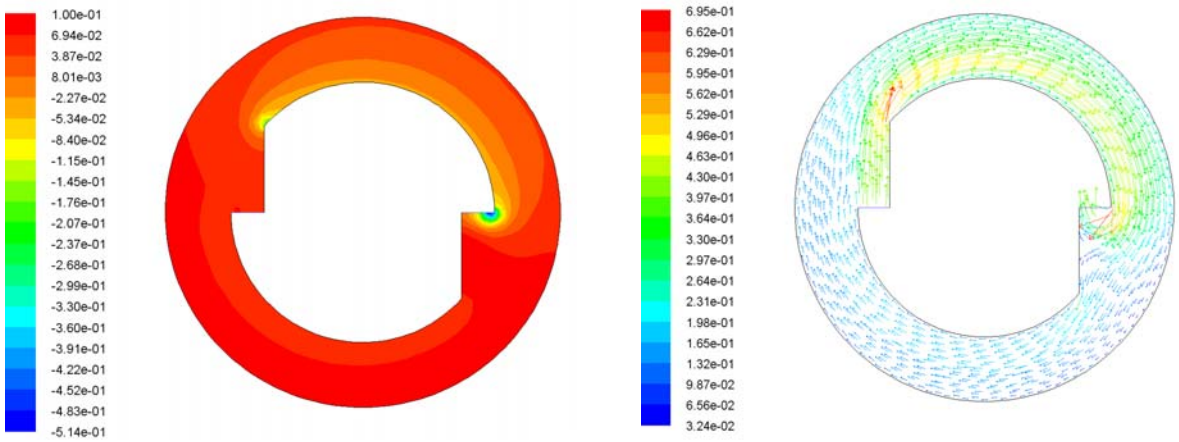

(a) The pressure field

(b) The velocity field

Fig. 16: The results as vascular robot is under roll conditions

is relatively small; the velocity trend in the cross-section has opposite direction rotation trend, clockwise rotation, so can ensure the vascular robot rotates more stable.

CONCLUSION

Refers squid jet-driven model, a new jet-driven vascular robot is designed and its drive parameters is analyzed and numerical simulation, the following conclusions are obtained:

- A combination pattern of suction and jet is used, jet-driven structure of the vascular robot is designed, mainly includes: the upper and lower shell, micro-batteries, variable pump, radio control block, 12 suction nozzles, 24 2/2-way solenoid valves and operation mechanism and the connection between them is described.
- The propel force of the jet-driven, pressure inside of elastic capsule, propulsive efficiency and other parameters are analyzed, the propel force and the jet velocity is related to sectional area of the nozzle, the pressure is related to the jet velocity, drive efficiency is related to the jet velocity and swimming velocity of the robot, for the initial calculated, the propulsive efficiency is 41.6%. The flow path control method is given with the posture adjustment of vascular robot.
- The dynamics mesh technology is used to analyze flow state when the capsule contraction and expansion in the variable pump, the results show that the contraction and expansion of the variable pump could jet and suck liquid to achieve the purpose of driving the vascular robot. the flow field of vascular robot with straight and adjustment conditions is simulated, the pressure field and velocity field characteristics as the vascular robot is swimming straight, pitch, roll, are corresponding to the robot corresponds movement trend.

REFERENCES

Chen, B., S.R. Jiang and Y.D. Liu, 2010. Research on the kinematic properties of a sperm like swimming micro robot. J. Bionic Eng., 7(Suppl.): 123-129.

Du, W., 2008. SMA wire actuated Squid like jet propeller prototype. MA Thesis, Dissertation, Harbin Institute of Technology, Harbin, China.

Jiang, F., 2010. A vascular robot dived by jet. Chinese Patent, No. 2010299445.6

Jiang, F. and H. He, 2012. Numerical optimization of cylinder flow structure of CO_2 laser. Res. J. Appl. Sci. Eng. Technol., 4(10): 1268-1276.

Jiang, F., W.P. Chen and Y.Y. Li, 2008. Numerical evaluation of spatial structure of suspended bio carriers. J. South China Univ., Tech., 37(12): 75-79.

Jiang, F., C.L. Zhang, Y.J. Wang, 2010a. Mechanical behavior analysis of CDIO production blood vessel robot in curved blood vessel. Lect. Notes Comput. Sc., 6377: 541-548.

Jiang, F., J. Yu and Z.W. Liang, 2010b, New blood vessel robot design and outside flow field characteristic. Appl. Mech. Mater., 29-32: 2490-2495.

Jiang, F., J. Yu and Y.J. Wang, 2010c. Influence of contractive and dilative motion of blood vessel to robot. Adv. Mat. Res., 139-141: 881-884.

Jiang, F., C.M. Huang, Z.W. Liang and Y.J. Wang, 2010d. Numerical simulation of rotating cage bio reactor based on dynamic mesh coupled two phase flow. Lect. Notes Comput. Sc., 5938: 206-211.

Jiang, F., J. Yu and Z.M. Xiao, 2010e. Outside flow field characteristic of biological carriers. Adv. Mat. Res., 113-114: 276-279.

Kim M.C., H.K. Kang and H.H. Chun, 2008. Simulation for the propulsion of a micro hydro robot with an unstructured grid. Ocean Eng., 35(8-9): 912-919.

Li, Z.G., 2008. Research on magnetic driving characteristic of a capsule micro robot. MA. Thesis, Dissertation, Dalian University of Technology, Dalian, China.